



**HAL**  
open science

## Effect of the lubrication between the tube and the die on the corner filling when hydroforming of different cross-sectional shapes

Abir Abdelkefi, Noamen Guermazi, Nathalie Boudeau, Pierrick Malecot,  
Nader Haddar

### ► To cite this version:

Abir Abdelkefi, Noamen Guermazi, Nathalie Boudeau, Pierrick Malecot, Nader Haddar. Effect of the lubrication between the tube and the die on the corner filling when hydroforming of different cross-sectional shapes. *International Journal of Advanced Manufacturing Technology*, 2016, 87 (1), pp.1169-1181. 10.1007/s00170-016-8552-1 . hal-01446415

**HAL Id: hal-01446415**

**<https://hal.science/hal-01446415>**

Submitted on 25 Apr 2023

**HAL** is a multi-disciplinary open access archive for the deposit and dissemination of scientific research documents, whether they are published or not. The documents may come from teaching and research institutions in France or abroad, or from public or private research centers.

L'archive ouverte pluridisciplinaire **HAL**, est destinée au dépôt et à la diffusion de documents scientifiques de niveau recherche, publiés ou non, émanant des établissements d'enseignement et de recherche français ou étrangers, des laboratoires publics ou privés.



Distributed under a Creative Commons Attribution 4.0 International License

# Effect of the lubrication between the tube and the die on the corner filling when hydroforming of different cross-sectional shapes

Abir Abdelkefi<sup>1,2</sup> · Noamen Guerhazi<sup>1</sup> · Nathalie Boudeau<sup>2,3</sup> · Pierrick Malécot<sup>2,3</sup> · Nader Haddar<sup>1</sup>

**Abstract** This paper presents an experimental study on corner filling in the tube hydroforming process. A single-step tube hydroforming process was retained based on pure expansion hydroforming with the conjunction of only internal pressure loading. Several hydroforming experiments were performed with differently shaped dies, such as a square, a rectangular, a trapezoidal, and a trapezoid-sectional die. The distribution of thickness was studied under both dry and lubricated conditions. The main results revealed that thinning occurred in the transition zone, between the corner radius and the straight wall, for both the square and rectangular dies. However, for the trapezoidal and trapezoid-sectional dies, the thinning took place in the sharp zone. The use of Teflon as a lubricant between the die and the tube led to significant changes in terms of thickness distribution and the reduction of thinning. For each of the various dies that were used, it was found that the lubrication of the contact tube/die offered a more uniform thickness for the final hydroformed product.

**Keywords** Square section · Rectangular section · Trapezoidal section · Trapezoid-sectional die · Lubrication effect · Thickness distribution

---

✉ Noamen Guerhazi  
noamen.guerhazi@enis.tn

<sup>1</sup> Laboratoire Génie des Matériaux et Environnement (LGME), Ecole Nationale d'Ingénieurs de Sfax (ENIS), B.P.1173-3038, Sfax, Tunisie

<sup>2</sup> Département Mécanique Appliquée, Institut FEMTO-STe, 24 rue d'Épitaphe, 25000 Besançon, France

<sup>3</sup> ENSMM, 26 rue d'Épitaphe, 25030 Besançon Cedex, France

## 1 Introduction

Compared with the more conventional punching and welding processes, tube hydroforming processes have the advantage of producing parts with fewer formative operations and a better quality of final products with complex profiles and various cross sections. It is important to note that, regarding this process, two cases can generally be distinguished. In the case of the “loading path,” the tube hydroforming process is used to conform the shape of the die cavity while simultaneously controlling the internal pressure and the axial feeding [1, 2]. As a result, the tube length can be changed. In the case of “pure expansion,” internal pressure is generally applied inside the tube while the tube length is kept constant during the test. However, if the tube is small enough to be directly placed into the die cavity, the forming process is then called “single-step hydroforming.” If the tube blank is too large for the die cavity to contain it, a “crushing process” will be needed before hydroforming [3, 4].

In the case of pure expansion hydroforming, based only on internal pressure loading, several authors have developed another specific test called the corner filling test, where a tube is expanded in a square section die. In 2003, Kridli et al. [5] experimentally investigated corner filling in a square section die. They also examined the thickness distribution against various measurement points for different locations. It was determined that the thickness distribution was relative to the corner radius and the strain-hardening behavior of the material. The thinnest zone, however, is located in the transition zone. Along similar lines, Hwang and Chen [6] have investigated the friction effect during an expansion test in a square section die. They examined the internal pressure against the corner radius, the variation of thickness at different stages, and the effect of lubrication. Furthermore, Liu et al. [7] have experimented with the thinning location in a square section;

the maximum thinning ratio was found to be about 25 %, and it occurred in the transition zone. Daly et al. [8] have studied the strain localization in tube hydroforming. Again, as reported in previous studies [5, 7], the thinning occurred in the transition zone. Xu et al. [1] have investigated the thickness distribution along the cross section of a square shape hydroformed part. It was found that the critical thinning took place in the transition zone, while the thickest element was located in the middle of the straight wall.

The effects of the friction coefficient, strain hardening exponent, and anisotropy coefficient on the thickness distribution have also been explored. For instance, Cui et al. [9] have studied the deformation of double-sided tube hydroforming in a square shape die. It was determined that for both internal and external pressure, the thinning always occurred in the transition zone, with little effect on the thickness distribution in the straight wall and the corner zone.

In the literature, significant efforts have been dedicated to studying the case of the rectangular section die. For instance, Yuan et al. [2] have studied the tube hydroforming without axial feeding in a rectangular section die. It was found that the thickness decreased gradually from the straight wall to the transition zone, and increased from the transition zone to the corner zone. According to Wang et al. [10], the plastic deformation first occurred in the transition point, and the equivalent strain of the transition point was consistently the largest. Moreover, different lubricants such as oil, molybdenum disulphide grease (Mso<sub>2</sub>), and polyethylene (PE) film were used to make the expansion easier. Some authors have also investigated hydroforming processes using other types of dies [4, 11]. For example, Xu et al. [11] have studied the hydroforming process in a trapezoid-sectional die, taking into account the effects of the friction coefficients and the thickness distribution. The main findings indicate that (1) a fracture occurred at the sharp corner, and wrinkling always occurred first at the obtuse corner; and (2) when the friction value increased, the uniformity of the thickness distribution decreased. In 2009, Li et al. [14] experimentally investigated crushing combined with subsequent hydroforming processes in a trapezoid-sectional die. Here, three factors were found to affect the uniformity of the thickness: the die closing seam, the tube diameter, and the performing load path. On the other hand, it was found that two kinds of defects could occur in the loading process: bursting was most liable to occur at the sharp angle, while wrinkling was most liable to take place at the blunt angle.

Contact at the interface tube/die was equally considered in both dry and lubricated conditions. The main objective when using good lubrication is to avoid some production problems such as buckling and wrinkling [12]. Ngaile et al. [13] have studied the lubrication mechanisms and their effects on interface friction, equally focusing on the lubricants' performances in the transition and

expansion zones for various geometries. Two kinds of tests have been used by Ngaile and colleagues to evaluate the lubrication effect: (1) the limiting dome height (LDH) test which is applicable to the transition zone, and (2) pear-shaped tube expansion (PET) which is applicable to the expansion zone. It was already shown [14] that lubrication reduces the frictional stresses of the tool–tube wall interface and helps to enhance product quality. To improve the formability in tube hydroforming by a reduction of friction, a specific lubricant was used in the research of Geiger et al. [15]. The lubrication here helped to reduce the friction effect and permitted a soft sliding between the tube and the tool surface. Not only were important sliding and homogeneous thickening obtained, but an increase of the wall thickness in the area close to the expansion zone was also achieved.

In 2008, Luege and Lucioni [16] experimented with the effect of lubrication on the thickness distribution. They have shown that the use of a lubricant led to the following: (1) the avoidance of any risk of crack; (2) an increase in the formability of the hydroformed tube; (3) an improvement in the tribological performance in the tube hydroforming process; and (4) an accurate prediction of the optimal use of this procedure for more complicated configurations.

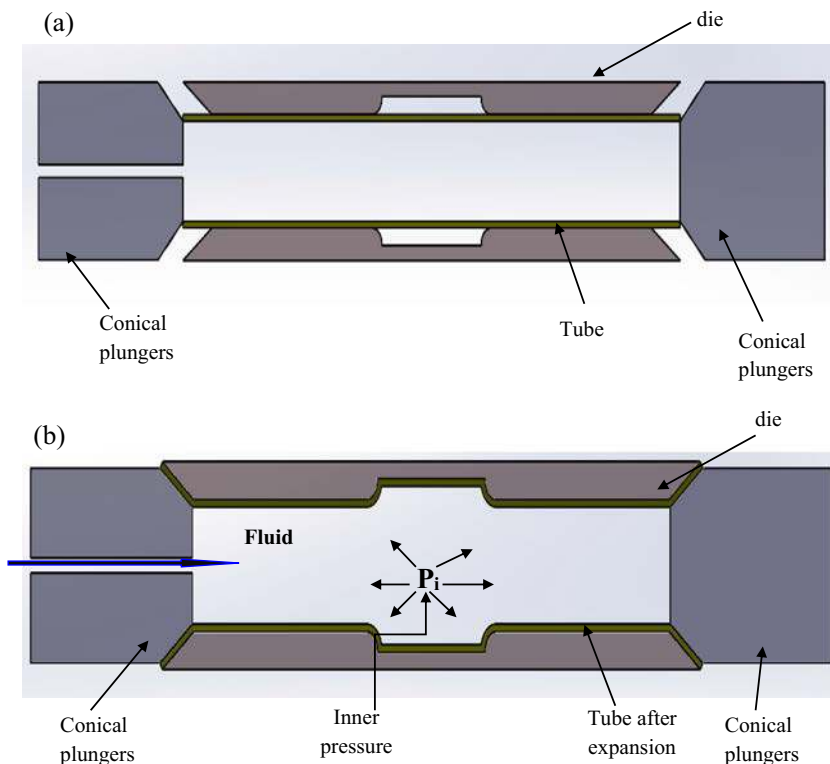
In this context, with the help of the “Aperam” industry (France), the aim of the present study was to build an experimental database with information about the relationship between the thickness distribution and the lubrication conditions when using differently shaped dies. The main motivation and innovation of the present paper consists of the study of the lubrication effect during corner filling in the case of pure expansion and “single-step tube hydroforming,” as shown in Fig. 1. Different shapes of hydroformed parts or section dies have been used, such as square, rectangular, trapezoidal, and trapezoid-sectional dies. For each configuration, the thickness distribution and thinning location were analyzed and evaluated with experimental measurements. The study also highlights the effect of Teflon as a lubricant at the interface tube/die. Finally, the differently shaped dies are discussed in terms of thinning reduction.

## 2 Experiments

### 2.1 Materials

The tube material studied in this work consists of deoxidized copper (Cu-DHP) with the following chemical composition (wt %): Cu 99.9 % and P 0.015 to 0.040 %. This K20/K21 Cu-DHP copper presents a limited residual phosphorus content, thus possessing excellent welding and hard soldering properties, as well as good resistance to hydrogen embrittlement. It also presents excellent formability and is used most

**Fig. 1** Definition of the different zones in tube hydroforming: **a** before expansion and **b** after expansion



effectively where requirements for electrical conductivity are not high. K21 presents a lower level of impurities compared to K20, making it possible to achieve a particularly low yield of strength values for a soft tube. The mechanical characteristics of this material can be found in Table 1. The dimensions of the tube samples are listed in Table 2.

## 2.2 The bulging test

The tube samples have been characterized with the tube bulging test, which is available at the FEMTO-ST lab (Fig. 2). The tube bulging test was chosen because it provides more appropriate material data for the tube than the classical tensile test [17–25].

**Table 1** Mechanical properties of the tube material

Density ( $\text{kg/m}^3$ )	8490
$R_m$ (MPa)	440
$R_{p0.1}$ (MPa)	420
A (%)	2
E (GPa)	132
Poisson's coefficient $\nu$	0.34
Strength coefficient K (MPa)	442
Strain hardening coefficient n	0.35
Yield stress $\sigma_Y$ (MPa)	80
Initial strain $\epsilon_0$	0.0075

## 2.3 The corner filling for the tube hydroforming process with various shapes

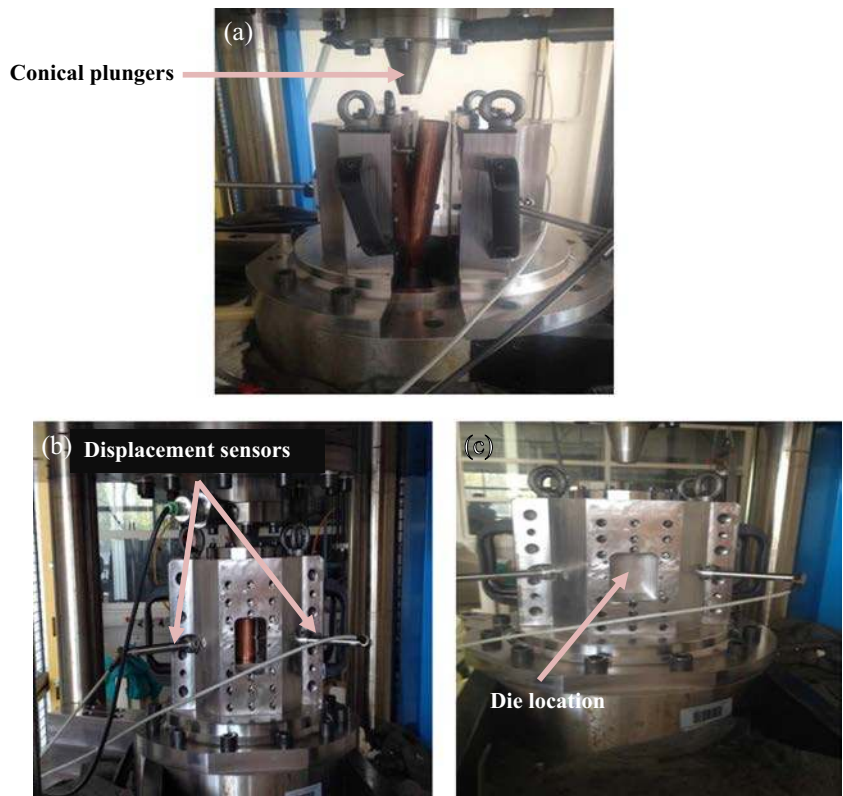
A modular tool was used for performing tube characterization in an open die as well as in a closed-shape die. This tool was installed with a hydraulic press available at the FEMTO-ST lab (Fig. 2). A multiplier pressure cylinder created high pressure in order to bulge the tube, and two vertical cylinders clamped the tube at its two extremities by cone-on-cone contact. The test proceeded as follows: (1) conical plungers came into contact with the ends of the tube and created a sealing effect by cone-on-cone contact; (2) the fluid was pumped inside the sample, resulting in a slowly increasing pressure; and (3) the tube deformed and progressively took the shape of the die.

Pure expansion as a single-step tube hydroforming process consisted of deforming a tube in a shaped die with the combination of internal pressure and fluid without axial feeding. At the beginning of the tests, some parameters needed to be adjusted, such as the maximal internal pressure, the sealing force that realizes the tube ends clamping, and the position of the displacement sensors. A displacement of 18 mm and a force of 40 kN were applied on the plungers, as previously

**Table 2** Dimensions of the tube samples

Length (mm)	External radius (mm)	Thickness (mm)
250	17.325–17.675	0.9–1.0

**Fig. 2** The modular tool installed on the press at the FEMTO-ST lab **a** before expansion, **b** during bulging test, and **c** during tube hydroforming process



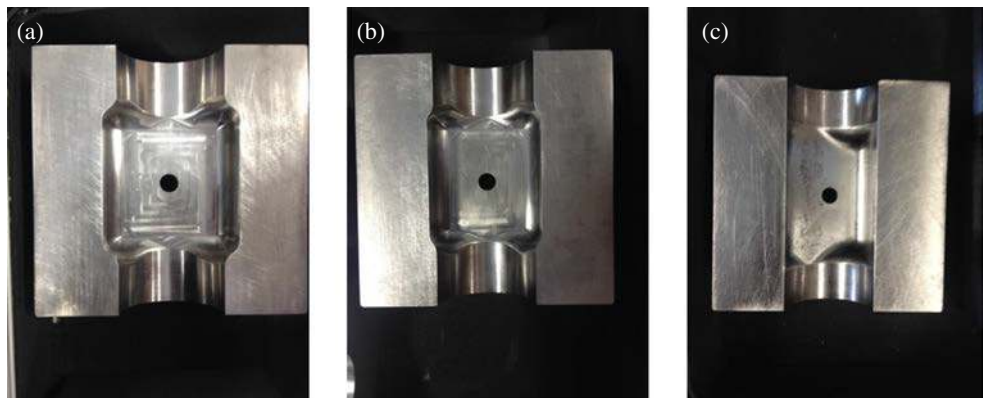
illustrated in Fig. 1. After that, a sealing force of 75 kN was applied during the hydroforming experiment to ensure the embedding of the tube.

As shown in Fig. 3, four models were considered: square, rectangular, trapezoidal, and trapezoid-sectional models. Only three die halves were presented, while the trapezoid-sectional model was a combination of square and trapezoidal shapes. The main dimensions of the differently shaped dies are given in Fig. 4. Also, as can be observed in Fig. 4, the initial tube is in contact with the square section at four points. However, for all of the other configurations, the initial tube is in contact with the die only at two points. Moreover, it is important to note that,

for each configuration, the perimeter of the final product is not the same as the perimeter of the initial tube.

Tube hydroforming experiments were performed under dry and lubricated conditions. A specific lubricant was used to evaluate the effect of lubrication on the tube hydroforming process; it is important to note that lubrication is a key factor that affects the tube's hydroformability. As a lubricant, "Teflon" was applied in aerosol form, which is generally used as a multifunctional grease for mechanical systems such as bearings, plain bearings, chassis joints, cams, rollers, chains, leaf springs, and cables, among other applications. Teflon provides numerous advantages, such as friction coefficient reduction, durability in extreme pressure, anti-wear protection, and

**Fig. 3** Shapes of the used dies: **a** square, **b** rectangular, and **c** trapezoidal



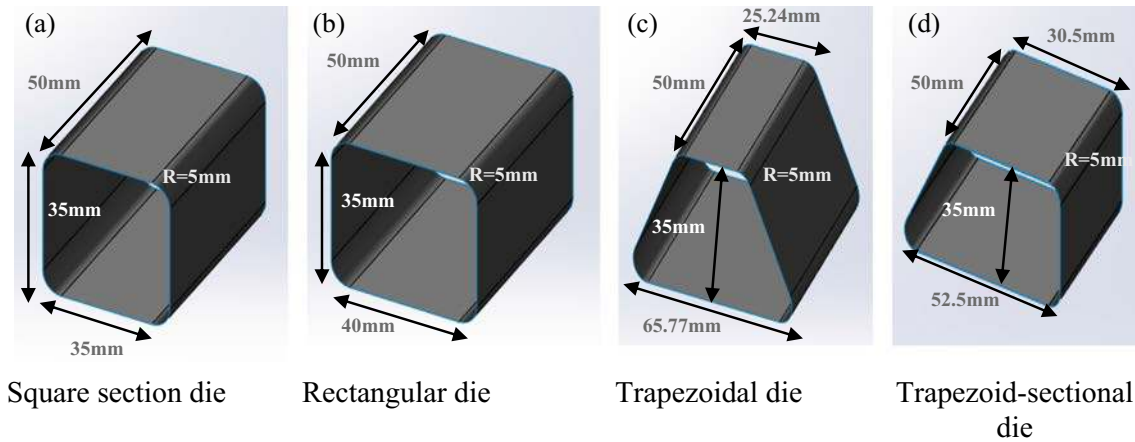


Fig. 4 Dimensions of square (a), rectangular (b), trapezoidal (c), and trapezoid-sectional (d) dies

good resistance to contact with water, steam, and many aggressive liquids. All of the relevant details of the lubricant are summarized in Table 3.

#### 2.4 Measures performed during the process

To study the forming behaviors of these different dies and the lubrication conditions, the tube expansion was controlled by three displacement sensors. During the hydroforming process, the internal pressure inside the tube and the tube deformation were measured. For tube deformation, three displacement sensors were placed in housing machines in the die as seen in Fig. 5. Each displacement sensor was placed at 120° to the next one. This allowed for plotting of the pressure–height expansion curve for the three displacement sensors. The point of the tube that was in contact with the first sensor was always the same throughout the process, while the points in contact with the other two sensors changed during the test. For the square and rectangular sections, three displacement sensors were used. However, for the trapezoidal and trapezoid-sectional dies, only two displacement sensors were considered (Fig. 5). The position of the displacement sensors was determined according to the work of Ouirane et al. [26] on the methodology of the bulging test.

Table 3 Details of the used lubricant “Teflon”

Physical state	Liquid, fluid, aerosol
Operating temperature	From -20 to 140 °C
Boiling point	77 °C
Density	<1
Water solubility	Unsolvable
Auto ignition temperature	200 °C
Point/Interval of decomposition	200 °C

#### 2.5 Measures performed on post-mortem tubes

It should be mentioned at this point that in this particular case, the tube hydroforming experiment could be interrupted at different pressure levels. The different samples were cut using the wire electrical discharge machining (EDM) process to avoid additional deformations of the tube due to the cutting process and to obtain precise contours. From these tube sections, it was possible to measure the outer and inner profiles. A contactless metrology machine (Werth IP 250) working with an image outline analysis was used. The sensor was a matrix analogic camera connected to a telecentric ×50 fixed lens, resulting in very precise repeatability ( $\pm 1 \mu\text{m}$ ). As the profile could not be measured in a single shot, the scanning method was used as illustrated in Fig. 6a. The machine automatically followed the sample’s profile and acquired a cloud of points. For each point, the part was illuminated and the image was treated as described in Fig. 6b. For each part of the hydroformed tube, the inner and outer profiles were measured, taking into account an average of 60 000 points. The data were saved as a text file that was analyzed with an original program to determine the thickness repartition along the profile.

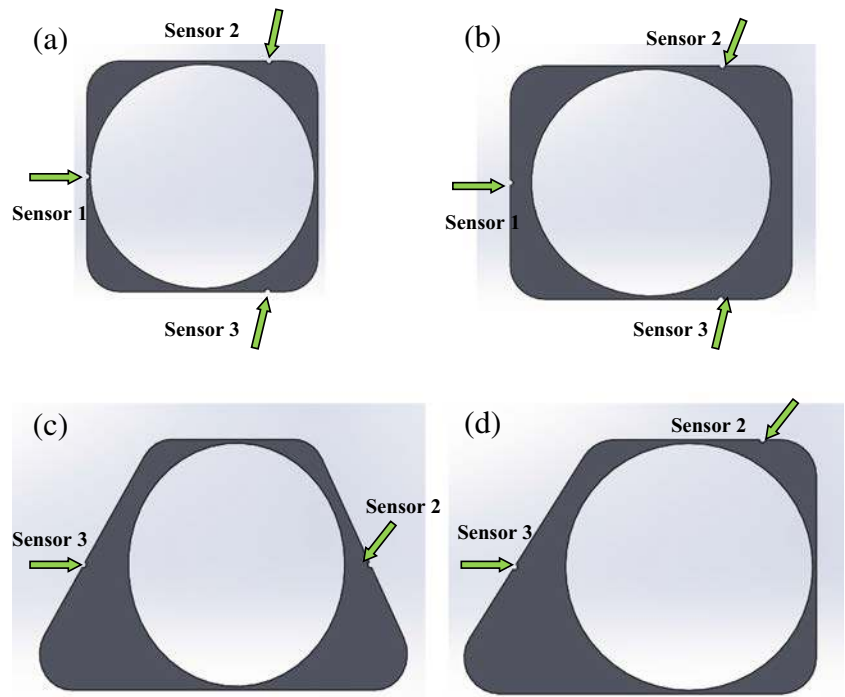
### 3 Results and discussion

In the following sections, the main results obtained will be presented with respect to (1) the thinning location under dry conditions, and (2) the lubrication effect on the thickness distribution for the differently shaped dies.

#### 3.1 Study of the thinning location in dry conditions

First, a preliminary study was conducted in order to determine the deformability of the tube samples to be tested in the hydroforming process. When samples were tested at their initial state, they did not display significant deformation. For this

**Fig. 5** Location of the three displacement sensors for the square (a) and rectangular (b) die and location of the two displacement sensors for the trapezoidal (c) and trapezoid-sectional (d) die



reason, the tube samples were subjected to a heat treatment before being tested again. In fact, all tubular samples were annealed at 450 °C for 30 min and then cooled in ambient air. Fig. 7 displays real photos of non-annealed and annealed tube samples after the bulging test. As can be clearly observed in Fig. 7, the annealed tube samples show remarkable ductility when submitted to internal pressure, even up to the onset of cracking.

As previously mentioned, during the bulging test, the applied internal pressure and the bulging height were regularly measured. These experimental measurements allowed for the pressure–bulge height curve to be plotted, as shown in Fig. 8a. Therefore, post-processing with the Boudeau–Malécot model [27] allowed for the stress–

strain curve and also the hardening curve to be determined, as shown in Fig. 8b. Here, Swifts law was considered, and Swifts parameters ( $K$ ,  $n$ , and  $\epsilon_0$  in Table 1) were determined based on the hardening curve.

With regards to Fig. 8a, b, which reveals the suitable behavior of the copper samples, the latter was tested in tube hydroforming. In this context, the four models were examined (square, rectangular, trapezoidal, trapezoid-sectional). It is important to note that for each shaped die, the focus was on estimating the maximal internal pressure which corresponded to full corner filling. Otherwise, when the tube was found to be embedded within the die, the single-step tube hydroforming test was stopped. With the same method, 28 and 28.5 MPa were revealed as the maximal internal pressure values for

**Fig. 6** a The scanning method available on the Werth IP 250 metrology machine. b The different steps of image treatment (Courtesy of Werth Messtechnik France)

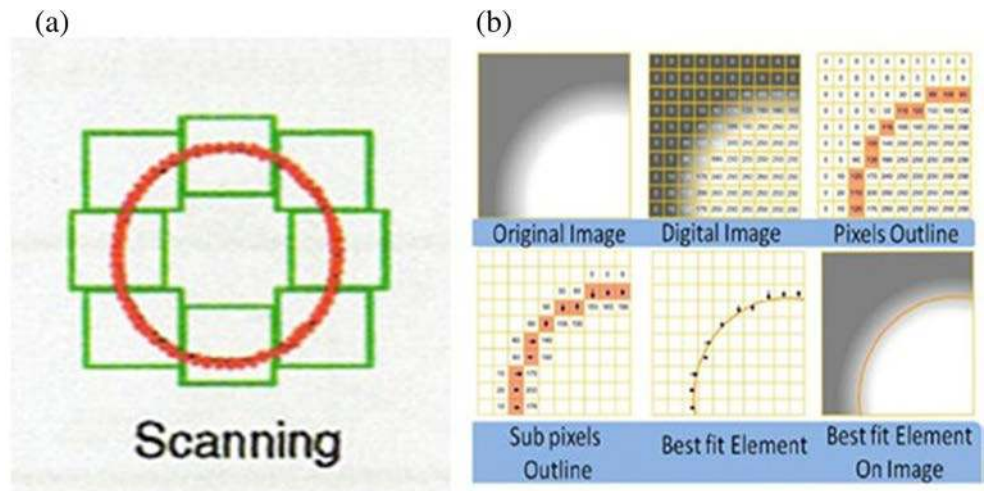




**Fig. 7** **a** Non-annealed copper tube and **b** annealed copper tube (exploded)

square and rectangular dies (Fig. 9). For trapezoidal and trapezoid-sectional models, a value of 16 MPa was determined.

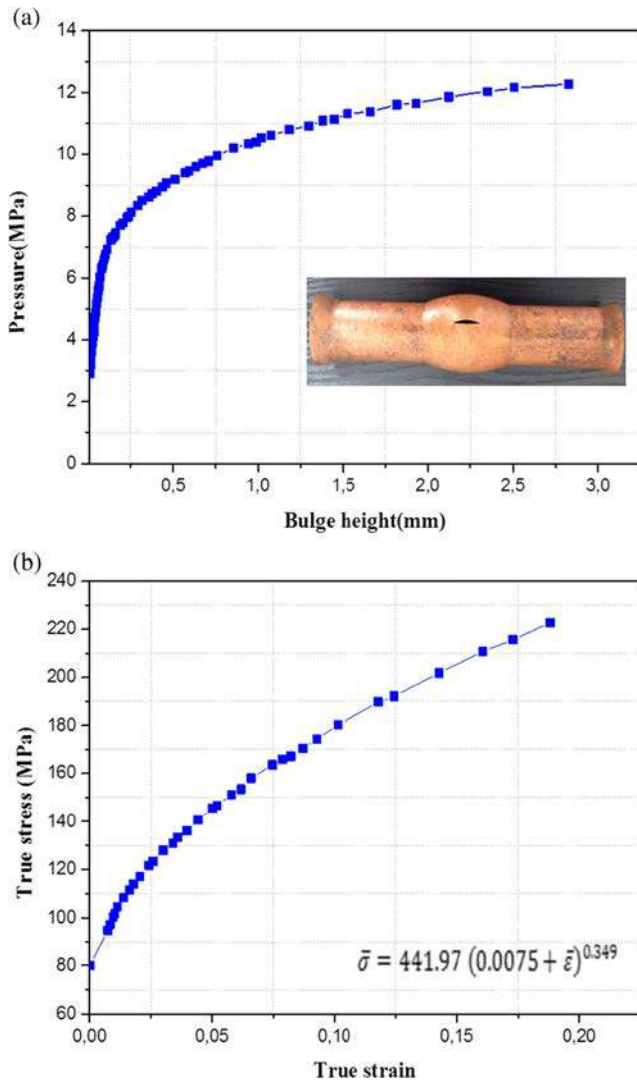


**Fig. 8** **a** Internal pressure—bulge height curve obtained from the tube bulging test. **b** The resulting hardening curve

The evolution of the internal pressure versus the displacement sensors for the differently shaped dies is shown in Fig. 10. All experimental tests were carried out without the appearance of cracks in the deformed tubes. It should also be noted that the displacement sensors (as presented in the  $x$ -axis in Fig. 10) consisted of the expansion of thickness (perimeter) and not the displacement of the tube according to the axial direction.

The main goal of this part was to define the thinning location for the differently shaped dies. For the square section die, the second and third displacement sensors, which were placed in the transition zone, achieved the same displacement (approximately 3 mm), and this was due to the symmetry conditions (as previously shown in Fig. 5). When corner filling was achieved, the thinning was stopped and the tube became embedded in the die. In this case, the bursting could not take place. However, the thinning occurred in the transition zone between the straight wall and the corner zone. For the rectangular section, the maximum displacement of both sensors corresponded to 5 mm. In this case, the location of the displacement sensors in the transition zone allowed for the prediction that cracking could take place by increasing the internal pressure.

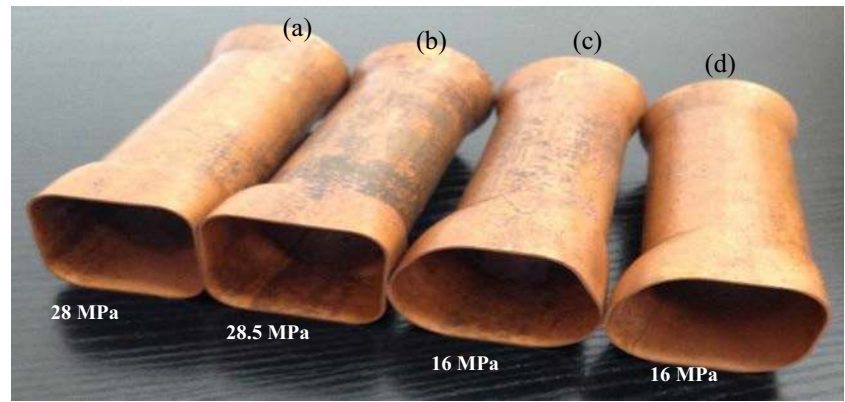
In the case of the trapezoidal die, the difference between the displacements obtained from both sensors was very significant: displacement values of 2.5 and 6.7 mm were recorded for the second sensor and the third sensor, respectively. Therefore, as the third sensor was placed at a sharp angle, an important thinning in this zone was expected.

For the trapezoid-sectional die, various kinds of angles were distinguished: a sharp angle ( $60^\circ$ ), an obtuse angle ( $120^\circ$ ), and two right angles. From Fig. 10, 1.8 and 6.6 mm were measured as maximum displacement values for the second sensor and the third sensor, respectively. Since the third sensor was placed in the sharp angle, the obtained displacement (6.6 mm) indicated that bursting could occur in the sharp angle.

In order to confirm the predictions presented above and to determine the precise thinning location, sufficient internal pressures were applied in order to attain the bursting stage of the tube. As previously explained, only the rectangular and trapezoidal shapes were considered. A-values of 16.5 and 29 MPa in terms of internal pressures were found to be responsible for inducing cracking for trapezoidal and rectangular shapes, respectively (Fig. 11).

According to Fig. 11a, it seems that matter first accumulated in the transition zone and then satisfied the yield condition because of the higher circumferential stress in the transition zone than in the corner and straight wall areas. Consequently, the deformation was accentuated in the transition zone. After that, necking occurred, progressively leading to the final fracture. The same observations were reported in the literature by Liu et al. [7]. Similarly,

**Fig. 9** Hydroformed tubes after expansion with various pressure values and different sections die: **a** square section, **b** rectangular section, **c** trapezoidal section, and **d** trapezoid-sectional



in the case of the trapezoidal shape (Fig. 11b), which has not yet been studied until now, it appeared that cracks occurred gradually along the longitudinal direction, eventually leading to the full bursting of the tube.

### 3.2 Study of the lubrication effect on the thickness distribution

In this section, a description is provided of the effects of lubrication between the tube and the die on corner filling during hydroforming of different cross-sectional shapes.

#### 3.2.1 Square section die

Figure 12 illustrates the thickness repartition along the transversal square section of the deformed tube. This repartition is represented only along a quarter of the section because of the symmetry conditions. Two cases have been discussed: tube hydroforming with and without lubricant. On the one hand, the experimental results exhibit that maximal thinning took place in the transition zone between the straight wall and the corner zone. This is in

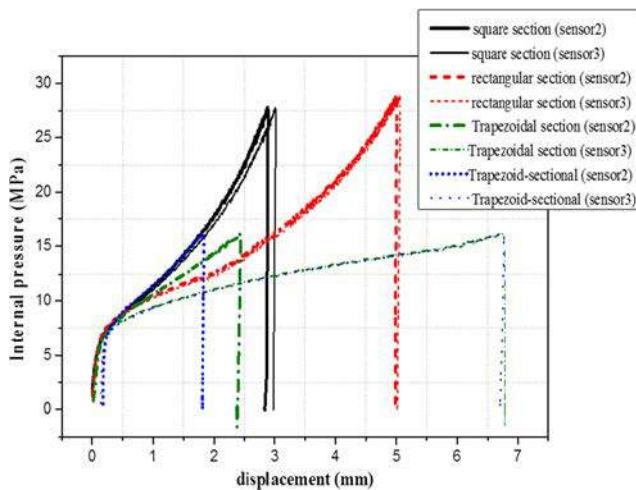


**Fig. 10** Evolution of the internal pressure against the displacement sensors for different sections die without lubricant

strong agreement with the observations of several other studies [7–10]. On the other hand, in order to discern the lubricant effect, the following formula was used:

$$\text{lubricant effect} \approx \frac{e_{\min}(\text{lub}) - e_{\min}(\text{dry})}{e_{\min}(\text{lub})} \times 100 :$$

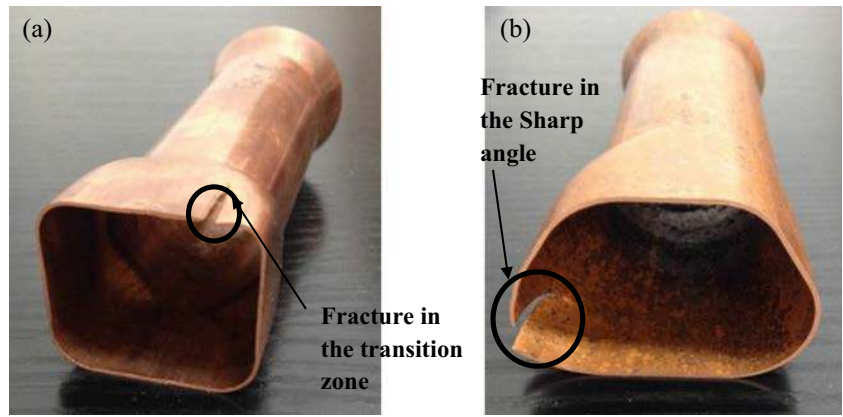
where  $e_{\min}(\text{lub})$  and  $e_{\min}(\text{dry})$  consist of the minimum thickness measured in the lubricated and dry conditions, respectively.

Accordingly, the lubricant played an important role in the reduction of thinning in the transition zone, point B, with 1.7 %. From A to B, the thickness decreased from 0.848 to 0.699 mm, while with the application of lubricant, it decreased from 0.853 to 0.716 mm. From B to C, the thickness increased from 0.699 to 0.82 mm, while with the lubricant, it increased from 0.716 to 0.843 mm. Therefore, the lubricant effect was found to be 2.3 % in the corner zone (point C). It can again be concluded that the lubricant softens the contact between the tube and the die. Consequently, it can be expected that the lubricant prevents any risk of crack or bursting and provides the most uniform thickness profile. In addition, it offers a better formability to the tube, as mentioned in previous research [15, 16].

#### 3.2.2 Rectangular section die

Figure 13 shows the variation of thickness along the transversal section of the deformed tube in the rectangular configuration. It is worth noting that this result was obtained under an internal pressure of 28.5 MPa without any risk of crack. In addition, only half of the tube had been considered due to the symmetry conditions. The thickness distribution was determined for four transition zones, two corner zones, and three straight walls. As was remarked in the discussion of the square configuration, in this case, the thinning occurred more significantly in the transition zone in comparison to the corner zone and the straight wall. This is in accordance with the observations reported in the literature [2, 10]. In particular, Yuan et al. [2] have

**Fig. 11** Bursting fracture of the deformed tube for: **a** rectangular and **b** trapezoidal section dies under maximal inner pressures of 29 and 16.5 MPa, respectively



shown that the thinning takes place essentially in the transition zone when focusing on stainless steel hydroforming. Wang et al. [10] have reported the same finding in their study about the hydroforming of an aluminum alloy tube with a rectangular section. However, it is clear from Fig. 13 that the use of a lubricant leads to an important reduction in thinning. For the test without lubricant, the maximum and the minimum thickness were 0.818 and 0.54 mm, respectively. Nevertheless, when a lubricant was used, it appeared that the thickness was less affected and the thickness distribution remained uniform. The maximum and the minimum thickness were 0.844 and 0.61 mm, respectively. For more explanation, the thickness reduction was estimated using the following formula, and the obtained results are summarized in Table 4:

$$\text{Thickness reduction (\%)} = \frac{e_0 - e_{\min}}{e_0} \times 100$$

where  $e_0$  is the initial thickness and  $e_{\min}$  is the minimal thickness obtained at the end of the test.

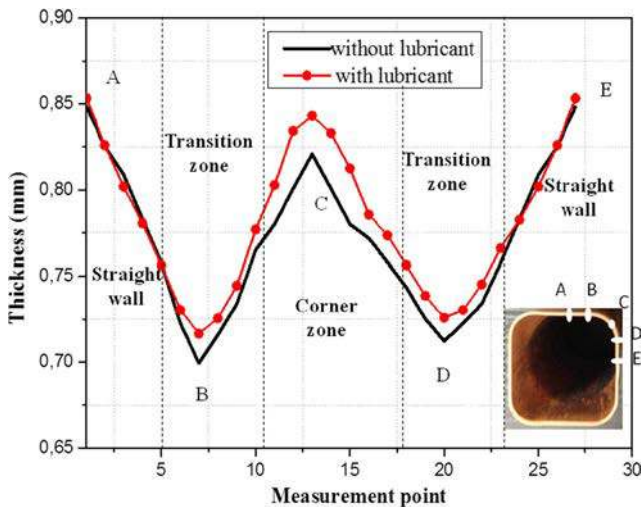


**Fig. 12** Effect of lubricant on the thickness distribution along the transversal section of the tube hydroformed using square section die (under an internal pressure of 28 MPa)

According to Table 4, it can be concluded that the maximum thinning always occurs in the transition zone at 39.9 %, against 24 % at the corner zone and 9 % at the straight wall. However, the use of lubricant reduces thinning from 39.9 to 32.2 % for the transition zone. The use of half of the model and not only a quarter of the model is to validate the same results of the first quarter and then to prove that the thickness reduction is unequal for the same position in the first and the second quarter. For example, the difference between both transition zones is approximately 5.6 %. However, with the use of the lubricant, we can notice that such difference is reduced from 5.6 to 1.5 %, which leads to the conclusion that the lubricant helps to provide uniform thickness. Finally, it is important to note that the thinning in the transition zone at the length of 40 mm was more significant than with the width of 35 mm (points B and H against points D and F).

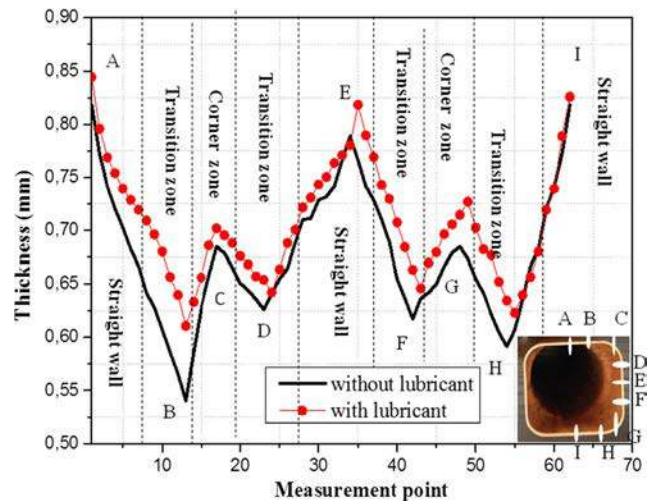


**Fig. 13** Effect of lubricant on the thickness distribution along the transversal section of the tube hydroformed using rectangular section die (under an internal pressure of 28.5 MPa)

**Table 4** Thickness reduction for rectangular section die

	Thickness reduction (%)								
	A	B	C	D	E	F	G	H	I
Without lubricant	9	39.9	24	30.4	12.3	31.4	23.9	34.3	9.1
With lubricant	8.4	32.2	22.1	28.6	9.1	28.3	19.3	30.7	6.3

### 3.2.3 Trapezoidal section die

Since there is no sufficient information about this kind of shape in the literature, the entire trapezoidal section was studied, as shown in Fig. 14. With a maximal pressure of 16 MPa, the expansion of the tube was achieved without any risk of crack. As shown in Fig. 14, the trapezoidal section was divided into four angles: two sharp angles and two obtuse angles. It is important to note that the main dimensions for both halves of the die were not similar, as can be observed in Fig. 5c. In the present study, the focus was on the evolution of the thickness distribution for different positions. Each point corresponded to a specific zone, and between them a critical zone such as B, D, F, and H. For point B, which presented the obtuse angle, the thickness decreased to 33.7 % for the dry test against 30.6 % for the lubricant test. For point D, which defined the sharp angle at this stage, the thickness reduction was found to be 37.48 % for the dry test against 36 % for the lubricant test. Concerning the second half on the right, for point F, which presented the sharp angle of the die, the thickness decreased to 19 % without lubricant against 18 % for the test with lubricant. For point H, which is defined by the obtuse angle, the maximum thickness reduction observed was 18 % for the dry test against 15.2 %

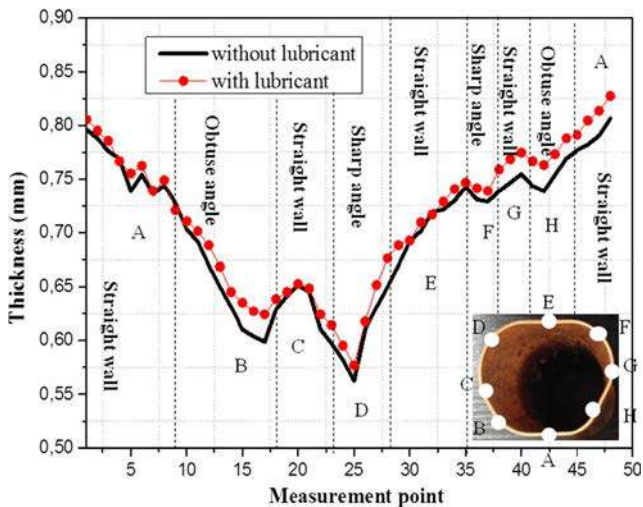


**Fig. 14** Effect of lubricant on the thickness distribution along the transversal section of the tube hydroformed using trapezoidal section die (under an internal pressure of 16 MPa).

for the lubricant test. For the other zones which correspond to the straight wall, including A, C, E, and G, the thickness reduction was 11.5, 27.6, 17.5, and 16.2 %, respectively, for the dry test, while the thickness reduction was 10.5, 27.5, 17, and 14 %, respectively, for the test with the specific lubricant.

Some general remarks can be made at this point. First, thinning was located in the sharp angle of point D with the highest thickness difference. This result is in agreement with those reported in the literature [4, 11]. However, a small difference is observed in the straight wall at point A. Second, the thickness difference decreased when a specific lubricant was used especially in the sharp corner with a reduction of 1.5 %. The effect of the lubricant was not similar for all zones of the trapezoidal section; it varied from 0.01 to 3.1 %. The minimum reduction was especially clear for the zone when the risk of thinning was lowest. Finally, the effect of the lubricant depended on the shape of the section, whether it was square, rectangular, or trapezoidal. The lubricant had an important impact in the rectangular die as compared with the trapezoidal die for the critical zone such as the transition zone (3.5 % as the lubricant effect) against the sharp angle with 1.5 %.

### 3.2.4 Trapezoid-sectional die

Figure 15 shows the thickness distribution along the transversal section of the tube deformed in the trapezoid-sectional die with an internal pressure of 16 MPa, both with and without lubricant. As can be seen in Fig. 15, the trapezoid-sectional model presented a sharp angle (60°), an obtuse angle (120°), and two right angles. The entire model had been examined,

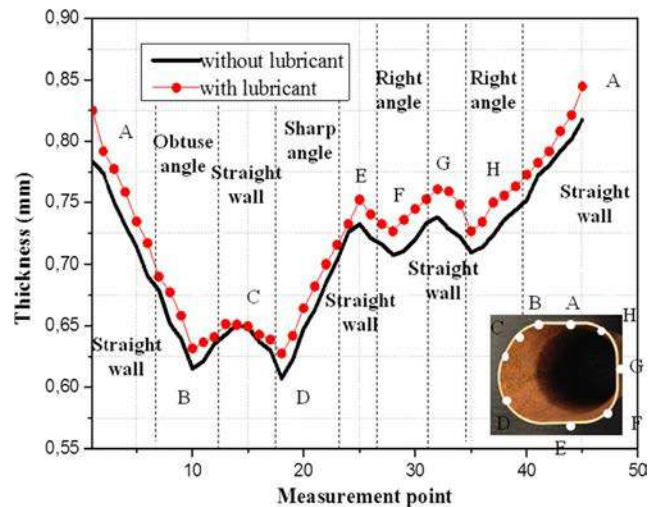


**Fig. 15** Effect of lubricant on the thickness distribution along the transversal section of the tube hydroformed using trapezoid-sectional die (under an internal pressure of 16 MPa)

and each point from A to H corresponded to a particular level of thinning reduction. The main findings revealed that the minimum thickness of the two parts was located in the sharp angle with 32.5 % thickness reduction for the dry test against 30.3 % for the lubricated test. Otherwise, the lubricant effect was estimated about 2.2 %. This result is in accordance with the observations reported in previous studies [4, 11]. In the second rank, the obtuse angle displayed 31.6 % of thinning for the dry test against 29.8 % for the lubricated test. In the third rank, the right angle presented a thickness reduction of 21.4 % for the test without lubricant against 19.33 % for the test with lubricant. In the final rank, the straight wall corresponded to the thickest zone. As usual, the lubricant helped to reduce the thinning for the various zones: the sharp angle, the obtuse angle, and the right angles with 2.2, 2.1, and 2.07 %, respectively.

### 3.2.5 A comparative analysis

From the thickness distribution shown in Figs. 12, 13, 14, and 15, the thickness variation ( $e_{\max} - e_{\min}$ ) can be calculated between the maximal thickness and the minimal one. As shown in Fig. 16, for the differently shaped dies, the thickness variation along the transversal section was compared. Here, it is important to note that since the results were obtained at different pressures, different amounts of expansion were expected, as were different thinning rates for the models. However, the main goals were (1) to study the thickness variation for each configuration and (2) to determine the shape that was the most affected by thinning in the final stage. The results obtained from the analysis of the data for the different shapes are summarized in Table 5. When considering the effect of the shape section on the thickness reduction, the rectangular section presented the

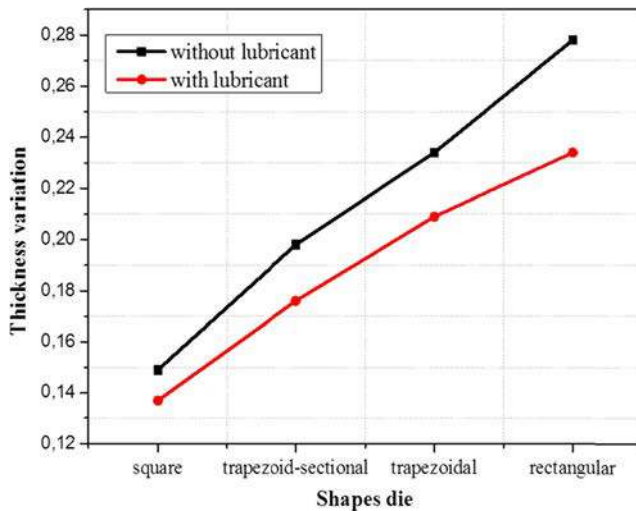


**Fig. 16** Thickness variation against the different shapes die for both hydroforming experiments conducted with and without lubricant

**Table 5** Thickness variation for different shapes die

	Thickness variation			
	Square	Rectangular	Trapezoidal	Trapezoid-sectional
Without lubricant	0.149	0.278	0.234	0.198
With lubricant	0.137	0.234	0.209	0.176

highest value of thickness variation with 0.278 and the square section displayed the lowest value with 0.149. The effect of the lubricant varied with the shape of the die. In fact, for all shapes, the thickness variation decreased with the use of lubricant. For example, it decreased from 0.149 to 0.137 for the square section. In addition, as can be seen from Fig. 16, the effect of the lubricant was more significant in the case of the rectangular section die. Here, it was assumed that the lubricant helped to enhance the metal flow without any risk of crack. Similar findings were reported by Kang et al. [12] when studying single-step hydroforming under dry and lubricated conditions and with various shapes of dies.

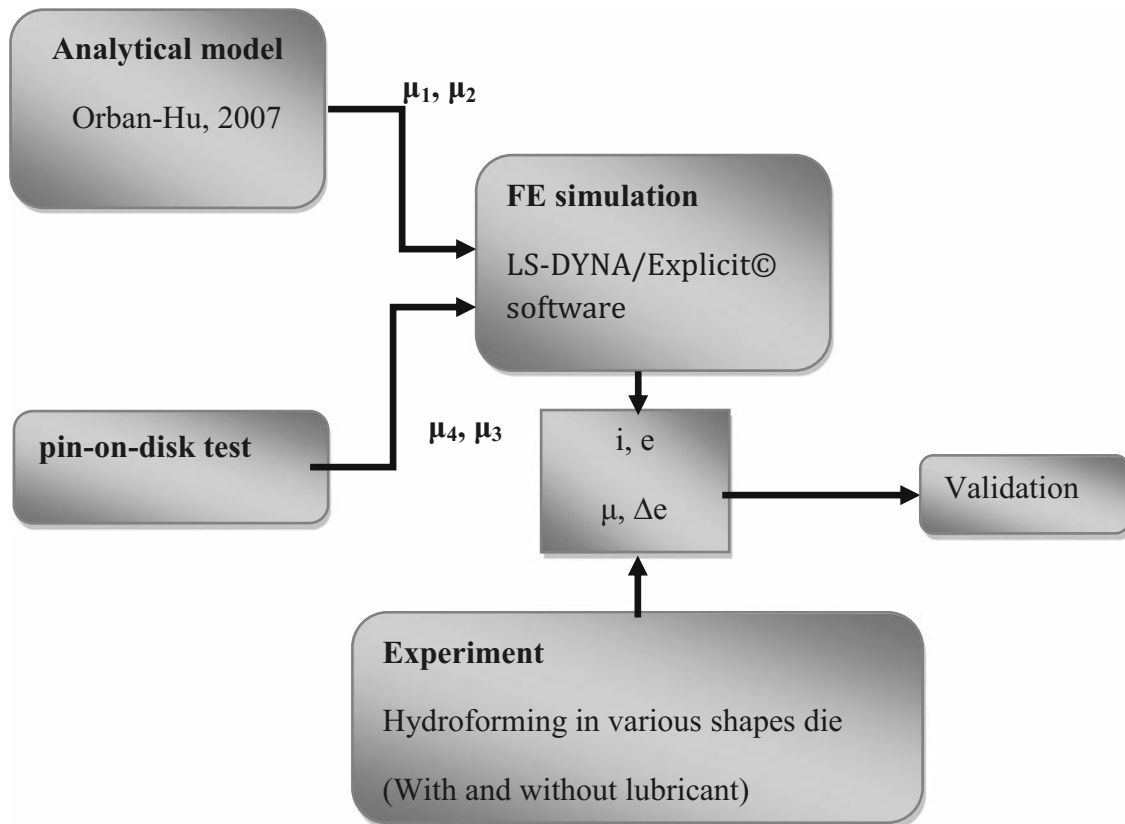
## 4 Conclusion

In this work, an experimental database for the relationship between the thickness distribution and the lubrication conditions when using differently shaped dies has been established. The following conclusions can be drawn from this study:

1. Under dry contact tube/die, the thinning location was found to be largely dependent upon the shape of the die. The thinning took place, for example, in the transition zone between the straight wall and the corner zone for both the square and rectangular sectioned dies. However, for the trapezoidal and trapezoid-sectional dies, the thinning occurred in the sharp angle.
2. The use of Teflon as a lubricant between the tube and the die played a significant role in the reduction of thinning.
3. Whatever the shape of the die, the lubrication of the contact tube/die offered a more uniform thickness for the final hydroformed product.
4. The thickness distribution along the transversal section of the deformed tube depended not only on the shape of the die but also on the nature of contact with the tube/die (i.e., dry or lubricated conditions).

Important insights have been revealed in this study, such as the following: (1) how to evaluate friction coefficient values from an analytical model and pin-on-disk test in order to run FE simulations, and (2) how to study the

validity of the characterized friction coefficient by performing both experiments and numerical simulations for the used shapes die. The following flow chart summarizes the possibilities for future research.



where:

- $\mu_1$  is the friction value obtained from the analytical model for the test without lubricant
- $\mu_2$  is the friction value obtained from the analytical model for the test with lubricant
- $\mu_3$  is the friction value obtained from the pin-on-disk for the test without lubricant
- $\mu_4$  is the friction value obtained from the pin-on-disk for the test with lubricant
- $i$  is the measurement point
- $e$  is the thickness
- $\Delta e$  is the thickness variation

**Acknowledgment** The authors thank Mr. Gerard MICHEL, mechanical engineer in the FEMTO-ST lab, for his help and contribution to this research.

## References

1. Xu X, Li S, Zhang W, Lin Z (2009) Analysis of thickness distribution of square-sectional hydroformed parts. *J Mater Process Technol* 209(1):158–164
2. Yuan SJ, Han C, Wang XS (2006) Hydroforming of automotive structural components with rectangular-sections. *Int J Mach Tools Manuf* 46(11):1201–1206
3. Nikhare C, Weiss M, Hodgson PD (2010) Die closing force in low pressure tube hydroforming. *J Mater Process Technol* 210(15):2238–2244
4. Li S, Xu X, Zhang W, Lin Z (2009) Study on the crushing and hydroforming processes of tubes in a trapezoid-sectional die. *Int J Adv Manuf Technol* 43(1–2):67–77
5. Kridli GT, Bao L, Mallick PK, Tian Y (2003) Investigation of thickness variation and corner filling in tube hydroforming. *J Mater Process Technol* 133(3):287–296
6. Hwang YM, Chen WC (2005) Analysis of tube hydroforming in a square cross-sectional dies. *Int J Plast* 21(9):1815–1833
7. Liu G, Yuan S, Teng B (2006) Analysis of thinning at the transition corner in tube hydroforming. *J Mater Process Technol* 177(1):688–691

8. Daly D, Duroux P, Rachik M, Roelandt JM, Wilsius J (2007) Modelling of the post-localization behaviour in tube hydroforming of low carbon steels. *J Mater Process Technol* 182(1):248–256
9. Cui XL, Wang XS, Yuan SJ (2014) Deformation analysis of double-sided tube hydroforming in square-section dies. *J Mater Process Technol* 214(7):1341–1351
10. Wang XS, Yuan SJ, Peng SONG, Xie WC (2012) Plastic deformation on hydroforming of aluminum alloy tube with rectangular sections. *Trans Nonferrous Metals Soc China* 22:s350–s356
11. Xu X, Zhang W, Li S, Lin Z (2009) Study of tube hydroforming in a trapezoid-sectional die. *Thin-Walled Struct* 47(11):1397–1403
12. Kang BH, Lee MY, Shon SM, Moon YH (2007) Forming various shapes of tubular bellows using a single-step hydroforming process. *J Mater Process Technol* 194(1):1–6
13. Ngaile G, Jaeger S, Altan T (2004) Lubrication in tube hydroforming (THF): part I. Lubrication mechanisms and development of model tests to evaluate lubricants and die coatings in the transition and expansion zones. *J Mater Process Technol* 146(1): 108–115
14. Ngaile G, Jaeger S, Altan T (2004) Lubrication in tube hydroforming (THF): part II. Performance evaluation of lubricants using LDH test and pear-shaped tube expansion test. *J Mater Process Technol* 146(1):116–123
15. Geiger M, Dal Bó P, Hecht J (2005) Improvement of formability in tube hydroforming by reduction of friction with a high viscous fluid flow. *Adv Mater Res* 6:369–376
16. Luege M, Luccioni BM (2008) Numerical simulation of the lubricant performance in tube hydroforming. *J Mater Process Technol* 198(1):372–380
17. Chen KK, Soldaat RJ, Moses RM (2004) Free expansion bulge testing of tubes for automotive hydroform applications (No. 2004-01-0832). SAE Technical Paper.
18. Koç M, Altan T (2001) On the characteristics of tubular materials for hydroforming—experimentation and analysis. *Int J Mach Tools Manuf* 41(5):761–772
19. Khalfallah A (2014) Experimental and numerical assessment of mechanical properties of welded tubes for hydroforming. *Mater Des* 56:782–790
20. Zribi T, Khalfallah A, BelHadjSalah H (2013) Experimental characterization and inverse constitutive parameters identification of tubular materials for tube hydroforming process. *Mater Des* 49: 866–877
21. Hashemi SJ, Naeini HM, Liaghat GH, Tafti RA (2015) Prediction of bulge height in warm hydroforming of aluminum tubes using ductile fracture criteria. *Arch Civil Mech Eng* 15(1):19–29
22. Teng B, Wang W, Liu Y, Yuan S (2014) Bursting prediction of hydroforming aluminium alloy tube based on Gurson-Tvergaard-Needleman damage model. *Procedia Eng* 81: 2211–2216
23. He Z, Yuan S, Lin Y, Wang X, Hu W (2014) Analytical model for tube hydro-bulging tests, part II: linear model for pole thickness and its application. *Int J Mech Sci* 87:307–315
24. He Z, Yuan S, Lin Y, Wang X, Hu W (2014) Analytical model for tube hydro-bulging test, part I: models for stress components and bulging zone profile. *Int J Mech Sci* 87:297–306
25. Zhang ZC, Manabe KI (2014) Influence of heat treatment on hydroformability of TRIP seamless steel tube. *J Iron Steel Res Int* 21(7):695–701
26. Boudeau N, Malecot P (2012) A simplified analytical model for post-processing experimental results from tube bulging test: theory, experimentations, simulations. *Int J Mech Sci* 65(1):1–11
27. Ouirane AHB, Boudeau N, Velasco R, Michel G (2011) Error evaluation on experimental stress–strain curve obtained from tube bulging test. *Thin-Walled Struct* 49(10):1217–1224